Nuclear Excitation by Scattering of 40-Mev Electrons*

W. C. BARBER, F. BERTHOLD,† G. FRICKE,‡ AND F. E. GUDDEN‡
High-Energy Physics Laboratory, Stanford University, Stanford, California
(Received August 1, 1960)

The electron energy spectra resulting from the scattering of 40-Mev primary electrons were measured for the purpose of studying nuclear excitations. Targets of Li^6, Be, C, and Si were employed at scattering angles of 132° and 160°; Pb was studied at a single angle of 160°. In addition to the elastic peaks, all spectra show peaks corresponding to excitation of the target nucleus into well-defined energy states. Peaks corresponding to known levels in Li^6 at 2.18 and 3.56 Mev, in Be^9 at 2.43 Mev, and in C^{12} at 15.1 Mev, were measured and analyzed by a virtual photon theory to give values of $(4_{-1.5}^{+3})\times10^{-4}$, 6.2±0.6, 0.13±0.03, and (40_{-6}^{+8}) ev for the values of their respective radiation widths to the ground states. Other well-defined peaks were observed at excitation energies of 16.9 Mev in Be, 11.6 Mev in Si, and 4.2 Mev in Pb. Broad peaks corresponding to the excitation of the giant resonance were observed in C, Si, and Pb, with maxima at 23, 20, and 15 Mev, respectively, and integrated cross sections of 75, 125, and 6500 Mev-mb, respectively. These cross sections are uncertain by a factor of approximately two because they depend on arbitrary methods used in subtracting the continuum of low-energy electrons and on arbitrary assumptions about nuclear form factors.

I. INTRODUCTION

THE interaction of an electromagnetic field with the nucleus can be described as a coupling of the externally produced scalar- and vector-potentials with the nuclear charge, current, and magnetization densities. If the electromagnetic field is that of a photon, its purely transverse vector potential is coupled with the nuclear currents and magnetic moments. If the field is produced by an electron, however, its Møller potential given by the initial and final electron states can be coupled in the Born approximation with the nuclear electromagnetic quantities. Whereas in the absorption of a photon by a nucleus the momentum transfer is fixed along the direction of the incident photon and is equal to the energy transfer,[1] in the electron process the momentum and energy transfer can be selected independently by proper choice of the electron scattering kinematics. This implies that in the photon process only matrix elements transverse to the momentum transfer can contribute, whereas in the electron process longitudinal matrix elements can contribute as well.

As long as the nucleus can be considered as a point, the cross section for electron excitation can be expressed in terms of the cross section for photon excitation without knowledge of the nuclear wave functions, except that the multipole order of the transition involved must be known. Theoretical calculations of the ratio of electron- to photon-excitation cross sections, approximating the nucleus as a point and the electrons before and after scattering as plane waves, have been made by a number of authors.[2–4] Calculations which include the effects of the finite nuclear size have been made by Schiff,[5] Dalitz and Yennie,[6] and Pal *et al.*[7,7a]

A number of experiments comparing photo- and electrodisintegration cross sections in the energy region of the giant resonance of the photonuclear effect have been reported.[8–10] In all these experiments the yields of reactions as a function of primary electron energy were measured, and the difficulties inherent in the photon-difference method limited the interpretation of the results.

Inelastic scattering of high-energy (100 Mev or greater) electrons has been used previously to study excited states of nuclei.[11–13] This paper presents some new results obtained using 40-Mev primary electrons from the Stanford Mark II linear accelerator.[14]

II. DESCRIPTION OF APPARATUS

The experimental setup was about the same as that described briefly[15] in connection with preliminary

* This work was supported by the joint program of the Office of Naval Research, the U. S. Atomic Energy Commission, and the Air Force Office of Scientific Research.

† On leave from Max-Planck-Institut für Chemie, Mainz, Germany.

‡ On leave from the Institut für Technische Kernphysik, Technische Hochschule Darmstadt, Germany.

[1] We use units such that $\hbar=c=1$.

[2] G. C. Wick, Ricerca sci. **11**, 49 (1940).
[3] J. S. Blair, Phys. Rev. **75**, 907 (1949).
[4] J. A. Thie, C. J. Mullen, and E. Guth, Phys. Rev. **87**, 962 (1952).
[5] L. I. Schiff, Phys. Rev. **96**, 765 (1954).
[6] R. H. Dalitz and D. R. Yennie, Phys. Rev. **105**, 1598 (1957).
[7] M. K. Pal, S. Fallieros, and R. A. Ferrell, Bull. Am. Phys. Soc. **4**, 229 (1959).
[7a] A formally complete calculation of the cross section for electron excitation of nuclei using the plane-wave approximation for the electrons has been given by Alder *et al.* [K. Alder, A. Bohr, T. Huus, B. Mottelson, and A. Winther, Revs. Modern Phys. **28**, 475 (1956)]. A calculation using approximate coulomb field-wave functions for the electrons has been made for electric and magnetic dipole transitions by R. Rodenberg, Z. Physik **158**, 44 (1960).
[8] K. L. Brown and R. Wilson, Phys. Rev. **87**, 962 (1952).
[9] R. L. Hines, Phys. Rev. **105**, 1534 (1957).
[10] W. C. Barber, Phys. Rev. **111**, 1642 (1958).
[11] J. H. Fregeau, Phys. Rev. **104**, 225 (1956).
[12] R. H. Helm, Phys. Rev. **104**, 1466 (1956).
[13] H. Crannell, R. Helm, H. Kendall, J. Oeser, and M. Yearian, Bull. Am. Phys. Soc. **5**, 270 (1960).
[14] R. F. Post and N. S. Shiren, Rev. Sci. Instr. **26**, 205 (1955).
[15] W. C. Barber and F. E. Gudden, Phys. Rev. Letters **3**, 219 (1959).

TABLE I. Parameters of the excited nuclear states that are observed by inelastic electron scattering. The transition energies denoted by asterisks in column (3) are assumed to occur only in the principal isotope of the target element.

(1) Target Element	Thickness (g/cm²)	(2) Spin and parity Ground state	Excited state	(3) Energy (Mev)	(4) Transition	(5) Scattering angle	(6) $\frac{\text{Area}_{\text{inelastic}}}{\text{Area}_{\text{elastic}}}$	(7) Estimated error	(8) $\int\sigma dk$ (Mev-mb)	(9) $\langle\int\sigma dk\rangle_{\text{av}}$ (Mev-mb)	(10) Γ_{exp} (ev)	(11) $\Gamma_{\text{exp}}/\Gamma_W$
Li^6	0.23	1^+	3^+	2.184*	$E2$	160°	2.6×10^{-3}	$+100\%$ -50%	6.0×10^{-4}	$(8_{-3}^{+6})\times10^{-4}$	$(4.1_{-1.5}^{+3})\times10^{-4}$	6
						132°	2.9×10^{-3}	$+100\%$ -50%	9.4×10^{-4}			
			0^+	3.560*	$M1$	160°	5.83×10^{-2}	$\pm10\%$	6.13×10^{-1}	$(6.2\pm0.6)\times10^{-1}$	6.2 ± 0.6	0.7
						132°	8.84×10^{-3}	$\pm20\%$	6.34×10^{-1}			
Be^9	0.211	$\frac{3}{2}^-$	$\frac{5}{2}^-$	2.43	$M1$	160°	1.14×10^{-2}	$\pm20\%$	1.18×10^{-1}	0.13 ± 0.03	0.13 ± 0.03	0.4
						132°	3.15×10^{-3}	$+75\%$ -50%	1.65×10^{-1}			
Be^9	0.376	$\frac{3}{2}^-$	? ? ?	16.9 ± 0.4	$E1$ $M1$ $E2$	160°	3.1×10^{-3}	$+75\%$ -50%	2.8 0.30 0.23	...	...	...
C^{12}	0.327	0^+	1^+	15.11*	$M1$	160°	1.12×10^{-2}	$+20\%$ -15%	1.88	$2.0_{-0.3}^{+0.4}$	40_{-6}^{+8}	0.55
						132°	1.97×10^{-3}	$+40\%$ -30%	2.44			
		Giant resonance		22.9	$E1$	160°	3.8×10^{-2}	$+100\%$ -30%	76	75.0_{-20}^{+60}	...	...
						132°	7.4×10^{-3}	$+100\%$ -50%	72			
Si^{28}	0.41	0^+	1^- 1^+ 2^+	11.6*	$E1$ $M1$ $E2$	160°	6.23×10^{-3}	$+30\%$ -20%	97 4.0 2.3	...	1030_{-210}^{+310} 47_{-9}^{+14} 16_{-3}^{+5}	0.66 1.4 7.5
		Giant resonance		20	$E1$	160°	1.26×10^{-2}	$+100\%$ -30%	125_{-40}^{+125}	...	...	...
Pb^{208}	0.075	0	1 1 2 3	4.14 ± 0.2	$E1$ $M1$ $E2$ $E3$	160°	2.1×10^{-3}	$\pm40\%$	880 16 1.9 0.0048	...	1230 ± 500 22 ± 9 1.6 ± 0.6 $(3\pm1.2)\times10^{-3}$	4.5 13 9 35
		Giant resonance		15	$E1$	160°	1.1×10^{-2}	$+100\%$ -50%	6500_{-3000}^{+6000}	...	...	...

results on inelastic scattering from C^{12}. The electrons from the accelerator were energy-analyzed in a double magnetic deflection system.[16] After passing through a secondary emission monitor, the primary electrons entered a scattering chamber. In its center they traversed a thin target, and then left the scattering chamber through a 0.0025-cm stainless steel window. The targets were of the order of 10^{-2} radiation length thick. Their exact thicknesses are given below in Table I. Detailed measurements were made at scattering angles of 132° and 160° only. At the 160° angle, all targets were placed normal to the incident beam except in the Li^6 and Pb experiments where the target was placed normal to the line bisecting the angle between the incident and scattered beams. For the 132° measurements with C, the target was again normal to the line bisecting the angle between the incident and scattered beams, but for the Be measurements the plane of the target contained the bisecting line. The latter situation yielded superior energy resolution because in this case the sum of the target distances traversed by the incident and scattered electrons is constant.

A double-focusing 18-in. magnetic spectrometer[17] analyzed the scattered electrons. The electrons were detected with two plastic scintillators forming a counter telescope as shown in Fig. 1. The output pulses of two RCA-6810 photomultipliers were fed directly into a coincidence circuit with 6-mμsec resolution. The spectrometer was calibrated at one field setting with 5.80 Mev α particles from Cm^{244}, and other momenta were determined by measuring the corresponding magnetic fields with a rotating-coil fluxmeter. This procedure resulted in a spectrometer momentum calibration of about 1% accuracy. The beam analyzing system was then calibrated to about the same accuracy by measuring the position of the elastic electron-scattering peak from a thin target. The energy spread of the beam, determined by slits in the analyzing system, was chosen in the range of 0.5% to 2%, according to the problem.

III. DATA COLLECTING AND ANALYZING PROCEDURES

The experimental method can be illustrated by the results in, for example, Fig. 2, which shows the C scattering data. The Mott scattering peak is at 41.6 Mev, with its radiation tail extending to lower energies. At 26.55 Mev there is a sharp peak representing the excitation of the 15.1-Mev 1^+ level in C^{12}, while in the region 18–20 Mev the giant resonance excitation is clearly seen. Target-out background has been subtracted from each measured point, a typical value being about 10% of the lowest target-in counting rate. The radiation tail results from two processes: radiation during scattering and radiation before or after scattering

[16] K. L. Brown, Rev. Sci. Instr. **27**, 959 (1956).

[17] Constructed with the aid of a grant from the Research Corporation.

in the electromagnetic field of a different nucleus. Processes other than radiation make a less important contribution to the tail. The occurrence of electron-electron scattering followed or preceded by wide-angle elastic scattering can, however, make a significant contribution.

(a) Radiation during scattering. The effect of this process was evaluated by Friedman[18] using the Schiff[19] calculation of the differential cross section for large-angle bremsstrahlung. Friedman's result can be written to give the ratio of the cross section $d^2\sigma_a/d\Omega dE$ for the inelastic scattering per unit solid angle and per unit energy interval at the final energy E to the Mott cross section $d\sigma/d\Omega$ for elastic scattering at the initial energy E_0. The result for the case that the nuclear recoil energy is small enough to be neglected is

$$\frac{d^2\sigma_a(E_0,E,\theta)/d\Omega dE}{d\sigma(E_0,\theta)/d\Omega} = \frac{\alpha}{\pi}\left(1+\frac{E^2}{E_0^2}\right)\left\{\ln\left[\frac{2E_0\sin(\theta/2)}{m}\right]-\frac{1}{2}\right\} \times\frac{1}{E_0-E}\left[1+\frac{E_0^2}{E^2}\frac{F^2(k)}{F^2(k_0)}\right], \quad (1)$$

where α is the fine-structure constant; m is the electron rest mass; and $F(k)$ is the nuclear form factor for Mott scattering with a momentum transfer k. For light nuclei and electron energies used in these experiments, the form factors can be approximated by

$$F^2(k)=1-\tfrac{1}{3}k^2\langle r^2\rangle, \quad (2)$$

where $\langle r^2\rangle$ is the mean-square radius of the nucleus.

(b) Radiation before or after scattering.[20] These processes contribute an effective cross section $d^2\sigma_b/d\Omega dE$ per unit solid angle per unit energy interval to the radiation tail, with a ratio to the Mott cross section given by

$$\frac{d^2\sigma_b(E_0,E,\theta)/d\Omega dE}{d\sigma(E_0,\theta)/d\Omega}=\frac{b(E_0,E)}{E_0-E}\left[t_i\frac{E_0^2}{E^2}\frac{F^2(k)}{F^2(k_0)}+t_0\right], \quad (3)$$

where t_i is half the target thickness (in radiation lengths) plus the full thickness of other material in front of the target, both taken in the direction of the incoming beam; t_0 is half the thickness of the target in the direction of the outgoing beam plus the full thickness of any material between the target and the spectrometer; and $b(E_0,E)/(E_0-E)$ is the bremsstrahlung number spectrum normalized to one radiation length for electrons of incident energy E_0 to produce photons of energy (E_0-E) in a unit energy interval. The order of magnitude of $b(E_0,E)$ is unity, but we have used the Bethe-Heitler thin-target spectrum including screening corrections for a more accurate value.

(c) Electron-electron scattering before or after elastic scattering. These processes are similar to those discussed under (b) in that two separate target atoms are required to produce the final result. The electron-electron scattering serves to produce lower-energy electrons, almost in the original direction, as the bremsstrahlung did in processes (b). The ratio of the effective cross section for this process to the Mott cross section is

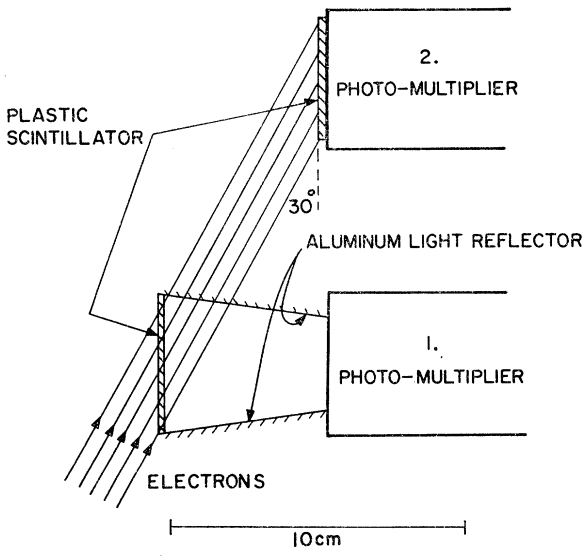

FIG. 1. Configuration of the coincidence telescope used for detecting the scattered electrons. The upper counter is in the focal plane of the spectrometer.

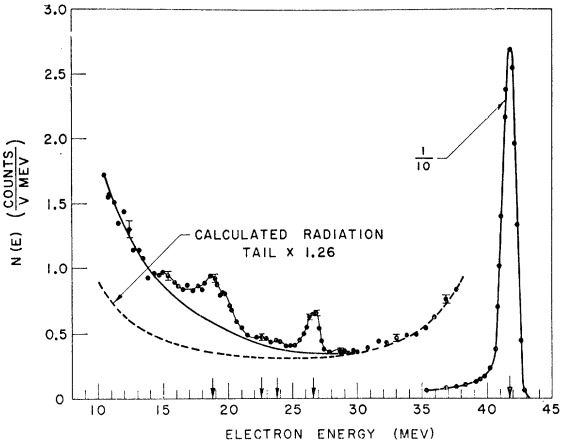

FIG. 2. Energy distribution of electrons, which were initially 42.5 Mev, after 160° scattering from a C target.

[18] J. I. Friedman, Phys. Rev. **116**, 1257 (1959).
[19] L. I. Schiff, Phys. Rev. **87**, 750 (1952).

[20] This process is also discussed in reference 18, but the result is presented in a slightly different form.

given by

$$\frac{d^2\sigma_e(E_0,E,\theta)/d\Omega dE}{d\sigma(E,\theta)/d\Omega}=\frac{d\sigma_{e-e}}{dE}\left[n_i\frac{E_0^2}{E^2}\frac{F^2(k)}{F^2(k_0)}+n_0\right], \quad (4)$$

where the Møller cross section is given by

$$\frac{d\sigma_{e-e}}{dE}=\frac{2\pi e^4}{mv^2}\left[\frac{1}{E^2}-\frac{1}{E(E_0-E)}\frac{m(2E_0+m)}{(E_0+m)^2}+\frac{1}{(E_0-E)^2}+\frac{1}{(E_0+m)^2}\right]; \quad (5)$$

and n_i is the number of electrons/cm^2 in t_i; n_0 is the number of electrons/cm^2 in t_0; and v is the velocity of the incident electron.

(d) Energy loss by ionization. This process produces a broadening of all the scattered peaks and a consequent loss of energy resolution. Because the probable energy loss is on the relativistic plateau, the broadening should be the same for all peaks. We have not made any corrections for this effect but have simply used the width of the elastic peak as an indication of the energy resolution, and the energy difference between elastic and inelastic peaks as a measure of the nuclear excitation energy.

IV. THEORY

The interaction of the electromagnetic field of the electron with the nuclear currents can be expressed most conveniently when the in- and outgoing electron waves can be represented by plane waves and when the nucleus can be approximated by a point. In this case there exist unique relations between the cross sections for electron-induced and photon-induced transitions, depending only on the multipole order of the transition. G. Kramer[21] has informed us that for the conditions of our experiment, where the products of nuclear disintegration are not detected, there should be no interference of electron waves scattered by different multipoles. For our experiments on light nuclei, the point approximation is fairly good, and we take this as the starting point of the analysis. The relation between the electron- and photon-induced cross sections may be written

$$\frac{d^2\sigma_e}{d\Omega dE}(E_0,k_f,\theta,l)=\frac{1}{k_f}\frac{dN_e}{d\Omega}(k_f,E_0,\theta,l)\sigma_\gamma(k_f). \quad (6)$$

This equation relates the nuclear absorption cross section $\sigma_\gamma(k_f)$ for a photon of energy k_f to the inelastic electron-scattering cross section $d^2\sigma_e/d\Omega dE$, where electrons of initial energy E_0 transfer the excitation energy k_f to the nucleus and are scattered through the angle θ into $d\Omega$, and into the energy interval dE at $E=E_0-k_f$. The factor relating the two processes, $(1/k_f)(dN_e/d\Omega)$, is called the virtual photon number spectrum any

[21] G. Kramer (private communication).

represents the angular distribution of inelastically scattered electrons for a given E_0, k_f, and multipole order l.

Dalitz and Yennie[6] discuss the calculation of the virtual photon intensity and show that it is convenient to write

$$\frac{dN_e}{d\Omega}=\frac{dN_e{}^t}{d\Omega}+\frac{dN_e{}^l}{d\Omega}, \quad (7)$$

where $dN_e{}^t/d\Omega$ results from matrix element components transverse to the momentum transferred to the nucleus, and $dN_e{}^l/d\Omega$ results from the longitudinal components of the matrix element. For electric transitions of multipole order l,

$$\frac{dN_e{}^t}{d\Omega}=\frac{\alpha}{4\pi^2}\frac{[p_0^2+p^2+p_0p(1-\cos\theta)]}{p_0^2(1-\cos\theta)}\times\frac{k_f^2}{k^2}\left(\frac{k}{k_f}\right)^{2l-2}\frac{F^2(k)}{F^2(k_f)}, \quad (8)$$

and

$$\frac{dN_e{}^l}{d\Omega}=\frac{\alpha}{2\pi^2}\frac{p^2(1+\cos\theta)}{k^2}\frac{2l}{l+1}\left(\frac{k}{k_f}\right)^{2l-2}\frac{F^2(k)}{F^2(k_f)}. \quad (9)$$

For the magnetic transitions the longitudinal components make no contribution, and the transverse contribution for a magnetic multipole of order l is given[22] by Eq. (8) with the factor $(k/k_f)^{2l-2}$ replaced by $(k/k_f)^{2l}$. In Eqs. (8) and (9), p_0, and p are the magnitudes of the electron momentum before and after scattering, respectively, and k is the magnitude of the momentum transferred to the nucleus ($k^2=p_0^2+p^2-2p_0p\cos\theta$). The factors $F^2(k)/F^2(k_f)$ are written explicitly to indicate that a correction for nuclear size might be required. These "form factors" depend on the nuclear wave functions of the initial and final states. Their determination would be of value in testing nuclear models, but our measurements are not accurate or extensive enough for this purpose. For the light nuclei we have studied, the form factors are close to unity; and we have analyzed the inelastic scattering using the approximation suggested by Barber[10]:

$$\frac{F^2(k)}{F^2(k_f)}=\frac{1-\frac{1}{3}k^2\langle r^2\rangle}{1-\frac{1}{3}k_f^2\langle r^2\rangle}. \quad (10)$$

Schiff's calculation[5] of inelastic scattering, which is not limited to the case $kr<1$, was carried out in detail only for the excitation of electric multipoles by the longitudinal components of the matrix elements. For this case the form factors are given by integrals over the transition charge density distribution.[23] The integrand

[22] We are indebted to Dr. G. Kramer (private communication) for the generalization of Eqs. (8) and (9) to multipoles of arbitrary order.

[23] It should be noted that Schiff's definition of the inelastic form factor is not exactly the same as the definitions implied by Eqs.

contains a spherical Bessel function of order equal to the multipole order of the transition. The series expansion of the Bessel function shows that although Eq. (10) is correct in order of magnitude, it tends to overestimate the correction when the multipole order is high.

In addition to the approximation $kr \ll 1$, Eqs. (8) and (9) are based on other approximations which should be examined. The initial and final electron states are taken as plane waves, and the interaction between the electron and the nucleus is treated to lowest order in α (i.e., only the exchange of one virtual photon is considered). Both of these approximations should be fairly good for light nuclei but not necessarily so for heavy ones. Brown and Wilson[8] and Barber and Wiedling[24] find discrepancies in the electrodisintegration of heavy nuclei which could be due to these approximations. In the case of magnetic transitions, Eq. (8) is subject to the additional uncertainty that the contribution of exchange currents can depend on the detailed nature of the nuclear interaction. An extension of the Siegert theorem[25] shows that the nature of the exchange currents does not affect the definition of charge density, and therefore the form of the electric multipole operators is unchanged. Hence, Eqs. (8) and (9) are to be regarded as more reliable for electric than for magnetic multipoles.

In the analysis of the data we have compared the inelastic scattering cross section with the elastic scattering cross section, i.e., the areas under an inelastic and the elastic peaks. The ratio is

$$\frac{\text{Area}_{\text{inelastic}}}{\text{Area}_{\text{elastic}}}=\left[\int \frac{dN_e}{d\Omega}\sigma_\gamma(k_f)\frac{dk_f}{k_f}\right]\left[\frac{d\sigma_{\text{point}}}{d\Omega}F^2(k_0)\right]^{-1}. \quad (11)$$

Equation (11) permits the analysis of the inelastic scattering in terms of the known elastic scattering cross section without the necessity of evaluating target thickness, solid angle of the spectrometer, fractional energy width of the counters, and beam-monitoring efficiency, because these quantities are the same for the inelastic and the elastic peak measurements. For the elastic cross section we have used the theoretical expression given by the first Born approximation. The elastic form factors $F(k_0)$ were computed from the nuclear radii given by Hofstadter.[26] This procedure should be adequate for the light nuclei we have studied. For the case of 160° scattering from C, for example, the Born-approximation cross section is 6.5% lower than the more correct McKinley-Feshbach formula.[27]

If $\sigma_\gamma(k_f)$ is a narrow resonance, $(1/k_f)(dN_e/d\Omega)$ can be considered constant and removed from the integral in Eq. (11). The equation can then be solved for the integrated photon absorption cross section.

If an inelastic scattering peak represents the excitation of a single level, its ground-state radiation width Γ_γ is connected to $\int\sigma_\gamma(k_f)dk_f$ by the Breit-Wigner formula which, for the photon case, is

$$\int\sigma_\gamma(k_f)dk_f=\pi^2\left(\frac{2I_c+1}{2I_g+1}\right)\left(\frac{1}{k_f}\right)^2\Gamma_\gamma, \quad (12)$$

where I_c and I_g are the spins of the excited state and the ground state, respectively.

V. MEASUREMENTS AND RESULTS

Measurements have been made to study the giant resonance region as well as the radiation widths and multipole types of transitions for individual levels.

There are two types of systematic experimental uncertainties which limit the accuracy of the present experiments, mainly in the giant resonance region.

The first problem is that the counter telescope efficiency is not independent of the electron energy. The efficiency becomes smaller for the lower energies, since electrons then have an increasing probability of being scattered through large angles by the first scintillator and therefore not hitting the second scintillator. An efficiency calibration was made by measuring elastic scattering from a Be target at different incident electron energies. The energy dependence of the measured cross section was compared to that predicted by the Mott formula with the necessary small form-factor corrections. The resulting efficiency calibration is shown by the points on Fig. 3. The efficiency was also calculated from the theoretical expressions for the multiple scat-

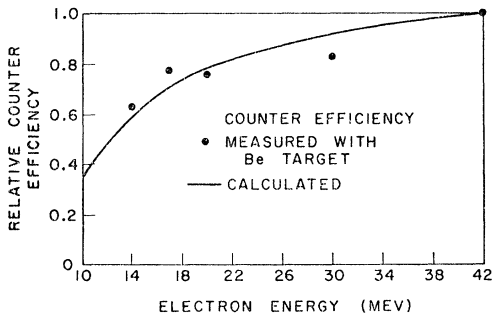

FIG. 3. Relative efficiency of the counter telescope shown in Fig. 1 as a function of electron energy. The experimental points and the calculated curve have been normalized to unity at 42 Mev. The experimental points have estimated errors of about 10%. The calculated curve was used in the analysis of all data.

(8) and (9). Schiff's definition is that the square of the form factor is equal to the actual integrated cross section for inelastic scattering divided by the theoretical elastic cross section for a point nucleus. The F^2 appearing in Eqs. (8) and (9) could be defined as the actual integrated cross section divided by what it would be in the limit as the transition multipole moments are shrunk to zero in dimension without changing the values of the moments.

[24] W. C. Barber and T. Wiedling, Nuclear Phys. (to be published).

[25] N. Austern and R. G. Sachs, Phys. Rev. **81**, 710 (1951).

[26] R. Hofstadter, *Annual Review of Nuclear Science* (Annual Reviews, Inc., Palo Alto, California, 1957), Vol. 7, p. 231.

[27] W. A. McKinley, Jr., and H. Feshbach, Phys. Rev. **74**, 1759 (1948).

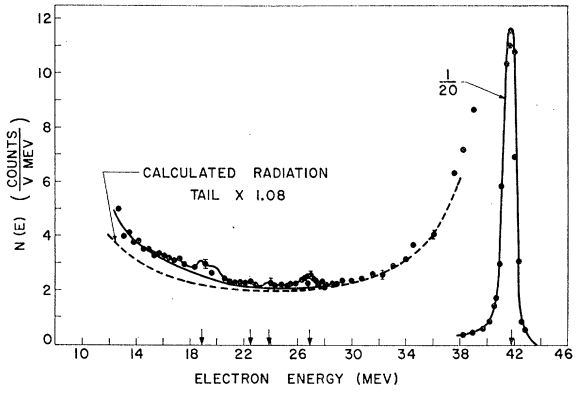

FIG. 4. Energy distribution of electrons, which were initially 42.5 Mev, after 132° scattering from a C target.

tering in the first scintillator and the known geometry of the counter telescope. The calculated efficiency arbitrarily normalized to unity at 42 Mev is shown as the solid curve in Fig. 3. The points fit the curve within the expected error of the calculation and the experiment. All data were corrected assuming the solid smooth curve gave the relative counter efficiency.

The second problem is that the low-energy tail is generally higher than the calculated radiation tail. For example, in Fig. 2 the calculated tail for the C scattering at 160° had to be multiplied by the factor 1.26 before it fit in the high-energy region. We do not know all the reasons for this disagreement, but an important contribution arises from the following mechanism: The electron beam diverges after passing through the target because of multiple scattering, so that a small fraction of the electrons does not leave the scattering chamber through the exit window but hits parts of the thick iron structure of the scattering chamber which are seen by the spectrometer. These electrons will scatter in the iron, and some of them will enter the spectrometer with degraded energy and yield a continuous spectrum that is not present in target-out background runs. The importance of this mechanism was proved by lining the critical parts of the scattering chamber with about 3 cm of paraffin. This removed roughly 30% of the unexplained electrons in the 15–20-Mev region. Also, Fig. 4 shows that the observed radiation tail agrees better with theory at a scattering angle of 132° than at 160°. This supports our hypothesis, because at smaller angles the spectrometer views a part of the chamber wall which is farther from the exit window.

These mentioned uncertainties make accurate area determination in the giant resonance region uncertain, but they have little effect on the observation of structures and their energy locations. Area determinations for sharp isolated peaks can be made satisfactorily.

The radiative corrections[28–30] affect the areas of both elastic and inelastic peaks. The correction for low nuclear excitations should be about the same fraction of the inelastic as of the elastic peak and hence cancel when the ratio, Eq. (11), is taken. All areas under peaks have been measured to an energy 2-Mev below the position of the peak. For high nuclear excitations (giant resonance region), the uncertainties discussed above are much larger than the radiative corrections, and the latter have been ignored in the analysis.

The energy spectra, corrected for the energy dependence of the counter efficiencies, are shown in Figs. 2, 4–7, 9, and 10. Most of the points represent averages of several runs, and the vertical lines shown on some of the points indicate typical standard deviations from counting statistics. Some data not shown in these figures include repeats of the Li^6 runs, a Si spectrum at 132°, and the low-energy portions of the Be spectrum.

The results of the analysis of the data are summarized in Table I. Column (1) lists the most abundant isotope of the target, and the mass per unit area of the target. All targets were natural mixtures of their isotopes except the Li target,[31] which was enriched to 95.7% Li^6. Columns (2), (3), and (4) list known or assumed data about the nuclear energy levels involved in the excitation process. Of the energy levels listed in column (3), those which are starred are presumed to occur only in the principal isotope of the element, and the data have been analyzed taking isotopic abundances into account. Giant resonances and the 4.2-Mev level in Pb are considered as more general features of nuclei, and in the calculations we have assumed they occur equally in all isotopes. Columns (5), (6), and (7) contain the experimental data. The errors listed in column (7) represent our estimate of the total experimental error, which in most cases results from difficulty in evaluating the area of the inelastic peaks. When the inelastic peaks are narrow and statistically well-defined, we have also considered possible errors due to target contamination and the error in the evaluation of the elastic peak.

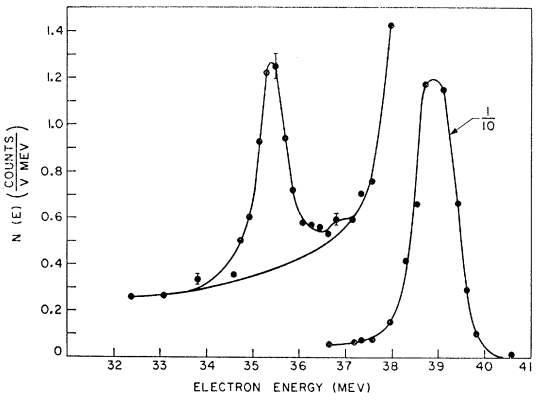

FIG. 5. Energy distribution of electrons, which were initially 39.5 Mev, after 160° scattering from a Li^6 target.

[28] J. Schwinger, Phys. Rev. **75**, 898 (1949).
[29] H. Suura, Phys. Rev. **99**, 1020 (1955).
[30] R. Hofstadter, Revs. Modern Phys. **28**, 224 (1956).

[31] We are indebted to R. Hofstadter for supplying this target.

Column (8) gives the integrated cross section for γ-ray absorption as calculated from Eq. (11). Column (9) is the weighted average of the values in column (8) for those cases where the same level was observed at two different angles. Column (10) gives the radiation width Γ_{exp} of the transition from the excited to ground state as calculated from Eq. (12). Column (11) gives the ratio of the widths in column (10) to the expected single-particle width Γ_W as given by Weisskopf.[32]

VI. DISCUSSION OF RESULTS

A. Li^6

This nuclide was studied with the intention of investigating the 3.56-Mev level; therefore, detailed measurements were made only in the neighborhood of the elastic peak. Figure 5 shows the results of a typical measurement at 160°. The elastic peak is at 38.9 Mev, and the peak at 35.3 Mev is the result of inelastic scattering with excitation of the 3.56-Mev level. The ratio of areas given in Table I is the average of four measurements which individually agree within 5%. The resulting value of 6.2 ev for the ground-state radiation width is estimated to have an error of $\pm 10\%$ because of possible systematic errors such as a small impurity on the target.

Since the present experiments were begun, the lifetime of the 3.56-Mev level has been measured by observing the elastic scattering of photons by the level with and without a Li^6 absorber in the primary beam.[33] The absorption experiment yielded a total width $\Gamma = (9.1_{-1.5}^{+2.0})$ ev corresponding to a mean lifetime of $(7.2_{-1.3}^{+1.5})\times 10^{-17}$ sec. The two experimental values of Γ disagree slightly, but in view of the preliminary state of the art of these measurements the difference is probably not significant. Kurath[34] has made calculations with intermediate-coupling wave functions and has found that the width is insensitive to the strength of the spin-orbit coupling. For the 35.6 Mev transition, he obtained a value of 8.35 ev at the LS coupling limit, 8.7 ev in the region where the energy spectrum matches the experimental one, and 8.8 ev for as large a spin-orbit coupling as is reasonable at the upper end of the 1p shell.

Figure 6 shows the results of the average of two runs at 132°. In addition to the inelastic peak at 35.3 Mev, there is a very small peak at 36.9 Mev that we interpret as resulting from the excitation of the 2.184-Mev level. Small bumps at this energy were also observed in the 160° runs. The analysis of these small peaks (Table I) yields a radiation width of $(4_{-1.5}^{+3.0})\times 10^{-4}$ ev, a result considerably higher than 3×10^{-5} ev obtained in a previous measurement.[35] A shell-model calculation by

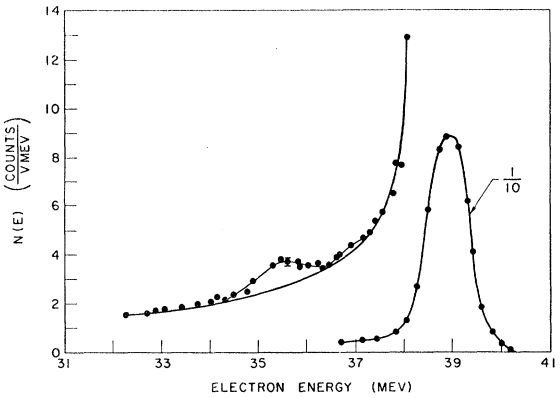

FIG. 6. Energy distribution of electrons, which were initially 39.5 Mev, after 132° scattering from a Li^6 target.

Kurath[36] gives 3×10^{-5} ev for the radiation width of this level. The disagreement of our result with the others is considerably greater than the estimated limits of error. We hope to make more measurements on this level in the future.

B. Be^9

The measurements near the elastic peak, Fig. 7, were taken with a rather thin (0.21 g/cm^2) target in order to maintain good energy resolution. The most significant inelastic peak occurs at a position indicating that it is primarily the result of scattering from the 2.43-Mev level. Although the determination of the area of the inelastic peak in the 132° measurements has a large uncertainty, this measurement combined with the 160° measurement is sufficient to rule out the possibility that the transition is electric dipole. Figure 8 shows the predicted angular dependence of the ratio of inelastic to elastic areas for three different types of transitions. The predicted increases in the area ratio in changing from 132° to 160° are factors of 1.2 for $E1$, 7.3 for $M1$, and 1.35 for $E2$ transitions. The observed increase is most likely 3.6 with limits of 1.7 and 8.6. An $M1$ assignment gives agreement with the experiment; and because the $E2$ virtual photon intensity is so much higher than that for $M1$, the permissible amount of $E2$ mixing is small. A mixture of 10% $E2$ intensity with 90% $M1$ intensity predicts an area ratio increase of 1.8 which is close to the experimental lower limit. The $E2$ intensity, therefore, cannot be much more than 10% and is probably less. The elimination of the possibility that the transition is $E1$ establishes the parity of the level as the same as the ground state. The spin assignments given in Table I, together with the measured area ratios, lead to a width of (0.13 ± 0.03) ev for the gamma transition to the ground state.

A suggestion of an inelastic peak at an excitation energy of about 4.2 Mev can be seen on the 160° data of Fig. 7. A slight bump at this excitation energy also

[32] J. M. Blatt and V. F. Weisskopf, *Theoretical Nuclear Physics* (John Wiley & Sons, Inc., New York, 1956), p. 627.
[33] L. Cohen and R. A. Tobin, Nuclear Phys. **14**, 243 (1959).
[34] D. Kurath (private communication quoted from reference 33).
[35] F. Däublin, F. Berthold, and P. Jensen, Z. Naturforsch. **149**, 208 (1959).
[36] F. Berthold (private communication).

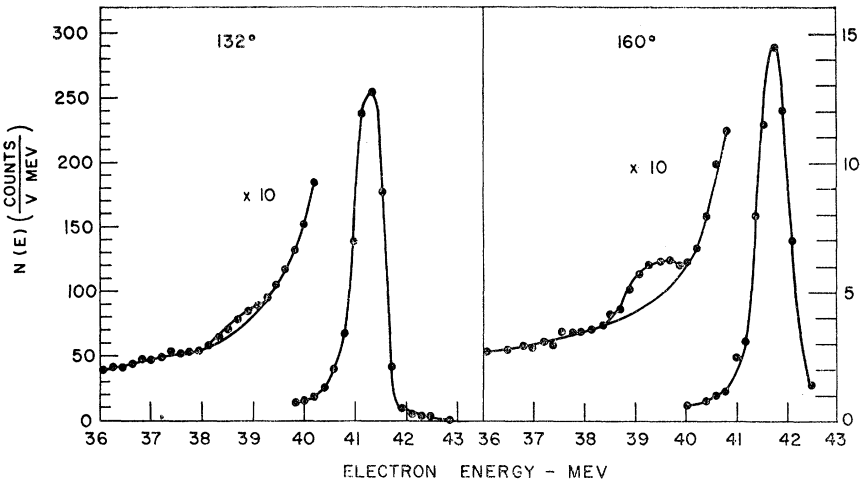

FIG. 7. Energy distributions of electrons scattered from Be at scattering angles of 132° and 160°. The primary electron energy was 42.5 Mev in both experiments, but in the 132° scattering the target angle was such that the electrons entered one side and left from the opposite side. This caused an increase in the energy loss in the target over that observed in the 160° experiment.

occurred in some measurements (described below) with a thicker target. Although there is no previous evidence for a level in Be^9 at this energy, our measurements lead us to believe that there is a 50% probability of its existence.

The region of low-energy scattered electrons, i.e., high excitation of the Be nucleus, was examined using a 0.38 g/cm² target at 160° only. Although the entire spectrum from 4-Mev to 23-Mev excitation energy was rather bumpy (curve not shown), the only peak we deemed worthy of measurement occurred at an excitation energy of (16.9±0.4) Mev. The data (Table I) do not permit any decision as to the multipolarity of the transition.

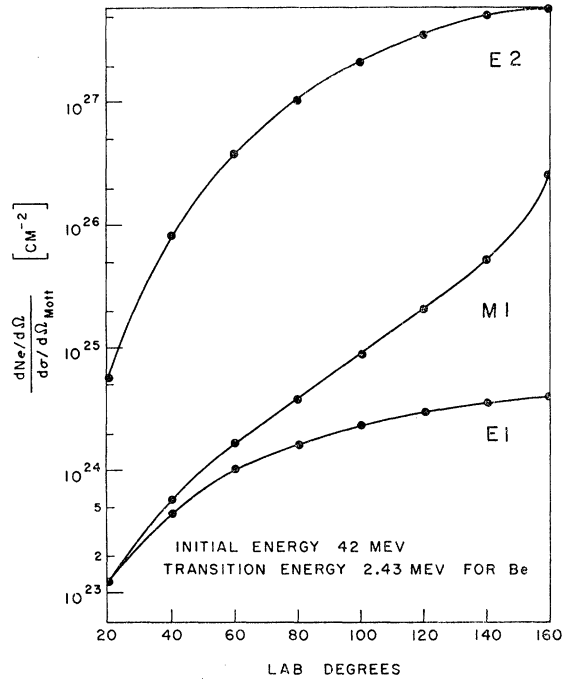

FIG. 8. The ratio of the intensity, Eq. (7), of 2.43-Mev virtual photons to the Mott scattering cross section from a point nucleus with $Z=4$ as a function of electron scattering angle. The three curves correspond to three different assumptions (electric dipole, magnetic dipole, and electric quadrupole) for the multipolarity of the 2.43-Mev transition.

C. Carbon

The C experiments consisted of repetition (with only slight changes in the experimental conditions) of the 160° measurements already reported,[15] and extension of the measurements to 132°. The new results, Figs. 2 and 4, have improved statistics and are significantly different from the previous ones only in that the evaluation of the energy dependence of the counter efficiency (Fig. 3) has raised the inelastic cross sections. The new value of (40_{-6}^{+8}) ev for the ground-state radiation width is somewhat lower than the values (54.5±9.3) and (59.2±9.7) ev obtained by elastic scattering of photons.[37,38] As in the case of the $M1$ transition in Li^6, our value of the radiation width is somewhat lower than the values obtained from x-ray experiments. This could be the result of errors in the virtual photon theory for magnetic transitions, but the disagreement is only slightly outside the estimated experimental errors, and the experimental errors would have to be reduced by an order of magnitude in order to make a conclusive test of the theory.

Peaks corresponding to the excitation of the giant resonance are exhibited at both scattering angles, but only at 160° are the statistics good enough to allow an examination of any structure in the peak. The maximum of the resonance is at an excitation energy of 23 Mev. The earlier measurements indicated a possible small peak at 22 Mev. In the new experiments this region was investigated by making five separate traversals of the spectrometer across the peaks. The average of the five runs (Fig. 2) indicates a small bump or shoulder at 22-Mev excitation. In the region between the 15.1-Mev peak and the main giant resonance there are two

[37] E. Hayward and E. Fuller, Phys. Rev. **106**, 991 (1957).
[38] E. L. Garwin, Phys. Rev. **114**, 143 (1959).

small bumps which are probably statistically significant because they can be seen in both Figs. 2 and 4. The excitation energies are (17.8±0.2) and (19.3±0.2) Mev. Known levels in C^{12} are plentiful in this region, but because of our poor resolution and statistics it is impossible to tell whether the small peaks result from individual levels or from combinations of several levels.

A reliable evaluation of the total area of the inelastic scattering from the giant resonance region is impossible, because we have no way to establish a baseline of scattering from non-nuclear effects. When the scattering peaks are narrow the baseline is fairly well defined, but the giant resonance is broad and its shape is not known in any detail. The areas we have used in evaluating the integrated cross section are those enclosed by the smooth curves shown as solid lines in Figs. 2 and 4. The smooth baseline curves are drawn arbitrarily, and it is only fortuitous that cross sections (Table I) derived from the 132° and 160° measurements agree so well. The average value of the integrated cross section up to 30-Mev excitation is (75_{-20}^{+60}) Mev-mb. This is, within the large error, in agreement with the sum of the measured values of the γ, n and γ, p cross sections.[39,40]

D. Si

The peak at 11.6-Mev excitation in the Si spectrum, Fig. 9, is probably caused by a magnetic-dipole transition. Electric dipole is unlikely because in this case the integrated cross section for γ absorption would have to be comparable to the giant resonance, and the level should have been observed previously in γ-ray experiments. Electric quadrupole is ruled out by the angular distribution; the level was not observed in the 132° spectrum, a result compatible with the $M1$ assumption but not with the $E2$. The size and position of the peak relative to the giant resonance are strikingly similar to the situation in C. This suggests that the 11.6-Mev peak is the Si^{28} analog of the 15.1-Mev C^{12} level. The magnetic-dipole assignment and the excitation energy are consistent with this idea.

The quantitative interpretation of the giant resonance in Si is subject to the same difficulties as in C. Our determinations of the position of the peak and the approximate size of the resonance are in agreement with a previous result.[41]

E. Pb

The Pb spectrum, Fig. 10, shows a small peak at 4.2 Mev and a "giant" resonance centered at 15 Mev. A peak at about 4.2 Mev has also been observed by inelastic scattering of 180-Mev electrons.[13] The high-energy measurements suggest an $E3$ assignment for the

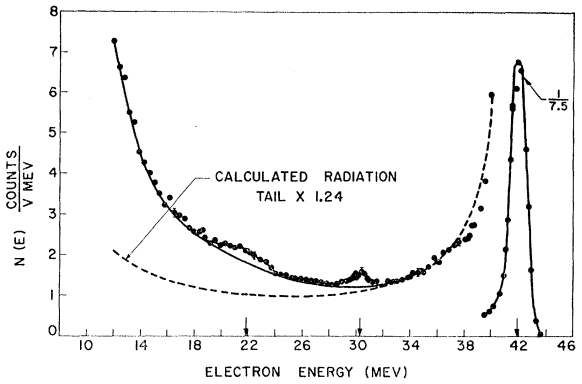

FIG. 9. Energy distribution of electrons, which were initially 42.5 Mev, after 160° scattering from a Si target.

transition and a radiation width of $(6\pm2)\times10^{-4}$ ev. A peak with the same form factor and the same excitation energy is also observed in the scattering from Bi^{209}. It is therefore believed that this level occurs in all the isotopes of Pb. Our result for the radiation width (Table I), assuming an $E3$ transition, is approximately six times larger. This suggests that different transitions are involved in the two experiments. The elastic peak, however, is greatly reduced by nuclear size effects. The square of the form factor is about 0.1 at 160°, and the approximate relation Eq. (12) can no longer be applied. The inelastic peaks will also be reduced by a form factor, and we have obtained the results in Table I under the arbitrary assumption that the form factor reduction is the same for the inelastic and the elastic peaks. The brief discussion in Sec. IV, based on the work of Schiff,[5] shows that this is not true: the higher multipoles are less affected by nuclear size. It is likely that in our experiment the inelastic form factor for the $E3$ transition is nearly unity. In this case, the value in Table I for the radiation width should be multiplied by the elastic form factor, and the result would agree with the high-energy experiment.

The analysis of the giant resonance under the assumption that elastic and inelastic form factors are

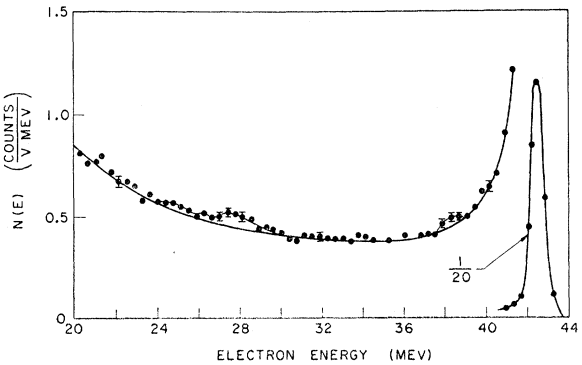

FIG. 10. Energy distribution of electrons, which were initially 42.5 Mev, after 160° scattering from a Pb target.

[39] W. C. Barber, W. D. George, and D. D. Reagen, Phys. Rev. 98, 73 (1955).
[40] L. D. Cohen, A. K. Mann, B. J. Patton, K. Reibel, W. E. Stephens, and E. J. Winhold, Phys. Rev. 104, 108 (1956).
[41] R. G. Summers-Gill, R. N. H. Haslam, and L. Katz, Can. J. Phys. 31, 70 (1953).

equal yields an integrated cross section of (6500_{-3000}^{+6000}) Mev-mb. The value from neutron yield measurements is 4800 Mev-mb.[42] Although the errors in our determination are large, we are gratified that we are able to make any measurement of the giant resonance in a heavy element where the elastic scattering is so strong. The fact that the ratio of the giant resonance peak to the elastic peak is about the same in Si and Pb suggests that when the experimental problem of the extraneous background is solved, the giant resonance in all elements can be investigated fruitfully by the method of inelastic electron scattering.

[42] R. Montalbetti, L. Katz, and J. Goldemberg, Phys. Rev. 91, 659 (1953).

ACKNOWLEDGMENTS

We wish to thank W. R. Dodge and G. Peterson for their help in constructing and operating the equipment. Three of us (FB, GF, FEG) wish to acknowledge the support of the German Bundesministerium für Atomkernenergie und Wasserwirtschaft, which made possible our stay at Stanford, and to thank Dr. W. K. H. Panofsky for his hospitality in making the facilities of the High-Energy Physics Laboratory available to us.

PHYSICAL REVIEW VOLUME 120, NUMBER 6 DECEMBER 15, 1960

Parameters of Some Low-Energy Neutron Resonances in Platinum*

JOHN R. WATERS†
Rensselaer Polytechnic Institute, Troy, New York
(Received August 5, 1960)

Measurements of the elastic scattering of neutrons from thin platinum foils were made as a function of neutron energy using a time-of-flight technique. Scattering areas were obtained for the 11.9, 19.6, 68, and 96-ev resonances. These were combined with a thick-sample transmission measurement and transmission data from other workers to give values for the parameters of the resonances. Level spins and partial widths were derived by a least squares method.

INTRODUCTION

MEASUREMENTS of the high-energy γ-ray spectra following neutron capture in platinum have been used to obtain values for the spins of the neutron resonances.[1–5] By combining this information with the results of transmission experiments, it is possible to arrive at other resonance parameters, such as the partial widths. However, the values obtained by this method are sometimes of poor accuracy due to the experimental uncertainty in the measured transmission areas. If neutron scattering measurements are performed, these data may be combined with the transmission areas to give an independent measurement of the level spin and also to obtain the other parameters with greater accuracy.

* Part of this work was supported by the U. S. Atomic Energy Commission.

† Now at the Physics Department, Princeton University, Princeton, New Jersey.

[1] J. R. Bird and J. R. Waters, Nuclear Phys. 14, 212 (1959).

[2] C. Corge, V-D. Huynh, J. Julien, S. Mirza, F. Netter, and J. Simic, Compt. rend. 249, 413 (1959), and Bull. Am. Phys. Soc. 4, 472 (1959).

[3] L. M. Bollinger, R. E. Coté, and T. J. Kennett, Phys. Rev. Letters 3, 376 (1959).

[4] M. K. Brussell and J. D. Fox, Bull. Am. Phys. Soc. 4, 34 (1959).

[5] M. K. Brussell and R. L. Zimmerman, Bull. Am. Phys. Soc. 4, 472 (1959).

METHOD

The experimental method has been described in detail before[6,7]; it consists, briefly, of the measurement of the elastic scattering of neutrons from thin samples of natural platinum as a function of neutron energy. A time-of-flight technique is used for the neutron energy determination. Thin samples must be used since the data are to be extrapolated to zero sample thickness to remove the effect of multiple scattering and self-absorption in the material. The combination of the resulting information with that obtained from neutron transmission experiments enables values of the spin of the excited level, J, the total, radiation, and neutron widths Γ, Γ_γ, Γ_N, respectively, to be obtained.

The scattering experiments were performed using the 15-Mev electron linear accelerator[8] at the Atomic Energy Research Establishment, Harwell, England, as a neutron source for time-of-flight measurements. An annular ring of 18 2-in. diameter by 16-in. long BF_3 counters was used as the detector with the sample at

[6] E. R. Rae, E. R. Collins, B. B. Kinsey, J. E. Lynn, and E. R. Wiblin, Nuclear Phys. 5, 89 (1958).

[7] J. R. Waters, J. E. Evans, B. B. Kinsey, and G. H. Williams, Nuclear Phys. 12, 563 (1959).

[8] M. J. Poole, and E. R. Wiblin, *Proceedings of the Second United Nations International Conference on the Peaceful Uses of Atomic Energy, Geneva, 1958* (United Nations, Geneva, 1958), Vol. 15, P/59.